ELSEVIER

Hybrid simulation study of ion escape at Titan for different orbital positions

I. Sillanpää [a,*], E. Kallio [a], P. Janhunen [a], W. Schmidt [a], K. Mursula [b], J. Vilppola [b], P. Tanskanen [b]

[a] *Finnish Meteorological Institute (FMI) Space Research, P.O. Box 503, FI-00101 Helsinki, Finland*
[b] *University of Oulu, Department of Physical Sciences, P.O. Box 3000, FI-90014 Oulu, Finland*

Abstract

Titan, the largest moon of Saturn, forms a unique plasma interaction with the Kronian corotating plasma. Titan's dense and nitrogen rich atmosphere is the primary source of the nitrogen torus around Titan's orbit through the subsonic and super-Alfvénic interaction between the corotating plasma of the Kronian system and the exosphere and ionosphere of Titan. We have studied this magnetic interaction of Titan with a global hybrid simulation model and especially the effect of the orbital position of Titan with four different Saturn local time. The hybrid simulation includes the various drifts important in Titan's plasma environment. Under the assumption of uniform magnetospheric properties along Titan's orbit, differences were found in the tail structure while the net emission rates varied only little. For all four studied orbital positions the magnetic field maximum was located on the anti-Saturn side of Titan. The iono- and magnetotails were co-aligned and tilted towards Saturn up to 45°.
© 2006 COSPAR. Published by Elsevier Ltd. All rights reserved.

Keywords: Saturn's magnetosphere; Titan; Induced magnetospheres; Plasma–ionosphere interaction; Nitrogen torus of Titan; Hybrid simulation

1. Introduction

The Kronian system of interacting moons, rings and magnetospheric plasmas is a rich and important object of study within the universe reachable by man-made probes. Hence the expectations for the Cassini (and Huygens) mission main phase have been building up (Blanc et al., 2002). The importance of the modelling efforts is perhaps all the more vital to the understanding of the physical mechanisms at work as the expected vast data yield from the measurements by the Cassini spacecraft has started to appear (e.g., Science, 13 May 2005 issue).

Titan's plasma interaction is unique in the known space (e.g., Neubauer et al., 1988). The attempts to model Titan's plasma environment have been hindered in the past by a lack of reliable atmospheric/exospheric models as only

little has been known despite Voyager 1's close flyby in 1980 (Hartle et al., 1982; Ness et al., 1982) and dedicated ground-based observations (e.g., Coustenis et al., 2003; Lellouch et al., 2003; Roe et al., 2004). Many results from various magnetohydrodynamic (MHD) models have been published over the last decade (Keller and Cravens, 1994a,b; Cravens et al., 1998; Kabin et al., 2000; Kopp and Ip, 2001; Nagy et al., 2001), but almost in all of them the need for hybrid simulations is recognized. This acknowledgement is in place as the kinetic effects are vital to the understanding of Titan's plasma interaction; the gyroradii are of the order of the radius of Titan (for ions H^+ and N^+ of the incident flow the values are 0.097 and 1.36 Titan radii, respectively). Although Brecht et al. (2000) produced hybrid model results, they used cold upstream plasma as did Ledvina et al. (2004) in their recent study. Thus, these models do not reflect well the plasma environment inside the Kronian magnetosphere, where the plasma near Titan is typically subsonic.

* Corresponding author. Tel.: +358 9 1929 2204; fax: +358 9 1929 4603.
  E-mail address: ilkka.sillanpaa@fmi.fi (I. Sillanpää).

This paper is about our results obtained with a global hybrid simulation model for Titan in a subsonic flow as measured by Voyager 1 in 1980 flyby. The description of the model parameters is given in the next section. In Section 3, we present results from simulations of four orbital positions where the direction of the ionizing ultra-violet radiation source varies accordingly. The recorded net outflows of ions are also given. These are followed by discussion and summary in Sections 4 and 5.

2. Model parameters

Our Titan model is based on a global quasi-neutral hybrid model developed for the study of the Mars–solar wind interaction (Kallio and Janhunen, 2001, 2002). In this section we will briefly go through the most important parameters of the simulation model, but will not dwell into the details of the model. For a more detailed view of the model we refer the reader to the above mentioned articles (see also Kallio et al., 2004). In the hybrid simulation, ions are represented as macroparticles moving under Lorentz force and electrons constitute a neutralizing, massless fluid. The magnetic and electric fields are also propagated self-consistently (the electron pressure term is not included in the algorithm at this stage).

The coordinate system in the simulation is chosen so that the X axis points against the flow direction of the ideal corotating plasma. The Y axis points from Saturn to Titan and the Z axis is northward thus completing the right hand coordinate system. The dimensions of the simulation box are as follows: $-20R_T < X < 12R_T$, $-24R_T < Y < 24R_T$ and $-20R_T < Z < 20R_T$ ($R_T = 2575$ km). The grid size varies to save computer time. The resolution is 1030 km ($= 0.40R_T$) in the area enclosing Titan and the tail structures ($-5R_T < X < 9R_T$); 2080 km in a layer with a width of 3–4R_T around the first area and finally 4120 km ($= 1.6R_T$) when $X < -12R_T$ or $X > 8R_T$ or $(Y^2 + Z^2)^{1/2} > 11R_T$. Titan and its exobase is represented by an obstacle boundary of radius $R_0 = 4175$ km (altitude of 1600 km). In this simulation the obstacle boundary is absorbing, e.g., a particle is removed from the simulation when coming in contact with the boundary. The area inside this boundary is fully conducting.

Our model includes three ion species. One singly charged ion species is taken to form the corotating plasma of the Kronian magnetosphere. The mass of this ion species is $m_i = 9.6m_p$ that comes from the average mass of nitrogen and hydrogen ions weighted with their corresponding abundances in the corotating plasma. This convention of a single species corotational plasma has been used by Kabin et al. (1999, 2000) in their 3-D MHD studies. The plasma inserted in the simulation box has density 3.0×10^5 ions/m³ with bulk velocity 120 km/s in the $-X$ direction and velocity distribution corresponding to the sound velocity $\sqrt{\gamma \frac{kT}{m_i}} = 199$ km/s that yields sonic Mach number $M_S = 0.6$ ($\gamma = 2$). This means that no shock forms around Titan as the flow is subsonic. The ambient magnetic field is taken to be 5 nT in the $-Z$ direction, i.e., southward. These physical simulation parameters reflect well the plasma environment around Titan according to the measurements during the Voyager 1 flyby (Neubauer et al., 1988).

There are two ion emission sources used, each with one ion species: one we call the ionospheric source for which we use ions of mass 28 m_p as of N_2^+ ions. Nitrogen molecules have the highest molar and mass fraction at the altitude of 1600 km according to models by Keller et al. (1992) and Amsif et al. (1997). Their emission takes place uniformly at the surface of the obstacle boundary at $R_0 = 4175$ km, which is reasonable as the density of N_2 quickly drops with altitude. We assume the ion density at this exobase altitude to be 3.4×10^7 ions/m³ and the ion temperature to be 1.0×10^5 K. The total ionospheric emission then becomes $q_{iono} = 1.6 \times 10^{25}$ ions/s.

The other ion emission source represents photo-ionization taking place at the exospheric neutral gas. We use a total ionization rate $f = 9.41 \times 10^{-8}$ s⁻¹ for forming singly charged ions of mass 16.01 m_p corresponding to methane ion CH_4^+. Methane is chosen as it has the highest density after 2000 km according to Amsif et al. (1997) and its mass is close to another important species N^+. This ionization rate is somewhat higher than that for methane from Huebner et al. (1992) taken to the distance of Saturn's orbit, but this is acceptable due to the limited number of ion species used as well as the absence of separate electron impact ionization in our simulations. For the exospheric density profile we use the Chamberlain density function

$$n(r) = n_0 \exp\left[\frac{GM_T m}{kT}\left(r^{-1} - R_0^{-1}\right)\right], \tag{1}$$

where m is the mass of a neutral methane molecule CH_4, M_T Titan's mass, $n_0 = 5.80 \times 10^{12}$ m⁻³ and $T = 186$ K. This is in accordance with the profiles presented by Amsif et al. (1997). The ionization rate with this density profile yields the total exospheric production rate $q_{exo} = 2.0 \times 10^{25}$ ions/s and 3.06×10^{25} ions/s for the case without shadow. The initial velocity of CH_4^+ ions (direction is random) is somewhat smaller than the excess energy of photo-ionization would give (Huebner et al., 1992) due to the limited number of macroparticles in the simulation. We made simulations with five different ionization configurations, four of them representing the four basic cases of a shadow for the solar extreme ultra-violet radiation (EUV), namely for Saturnian local times (SL) 0, 6, 12 and 18 h, and the fifth one with no such shadow. The case with no EUV shadow can be seen as an upper estimate for the electron impact ionization based on a study by Keller and Cravens (1994a, see also Keller et al., 1994b) as our simulation model uses no actual electron impact ionization.

The boundary conditions employed for the sides $X = -20 R_T$ and $X = 12 R_T$ are absorbing. The macroparticles of the flow are inserted randomly in the first layer of grid cells at the ramside, and particles are also inserted at the back wall ($X = -20 R_T$) to keep the density and the

bulk velocity of the unperturbed flow uniform throughout the simulation box. The boundary conditions at the sides parallel to the bulk flow are such that they mimic an ambient plasma with the proper bulk and thermal velocity; the ions impacting these sides are returned back with a velocity from that velocity distribution at a random place on the same or opposite side. This is done so that no net outflow occurs through the boundaries on these sides. However, the particles are returned in such a way only if they were of the species of the corotational flow, so that ions emitted at Titan are removed from the simulation once reaching the edges. Fully absorbing boundary conditions are out of question since the thermal speed exceeds the bulk speed.

The simulations were run for more than 3000 s; although it takes only about 700 s for the flow to fill the box, it takes some 2000 s for the ions emitted from Titan to migrate to the edges of the simulation box and for the tail structure to fully develop. About 1.44 million macro-

particles existed in the simulation box at any given instance.

3. Four cases of EUV direction

Here we present the results of our global hybrid simulations of Titan's plasma environment in the four basic cases of Titan's orbital position. It is important to note that only the exospheric methane CH_4^+ ion source changed according to the shadow of Titan on the exosphere, and that the ionospheric emission was not changed between these four cases. The differences become reasonably large. This is because the photo-ionization rate dominates the ion emission at Titan in our simulations ($q_{exo} > q_{iono}$) and thus the ion distribution varies considerably between the cases.

Fig. 1 shows the number density of the exospheric source ions (CH_4^+) and Fig. 2 the total magnetic field in the orbital plane in the four cases. The panels for different

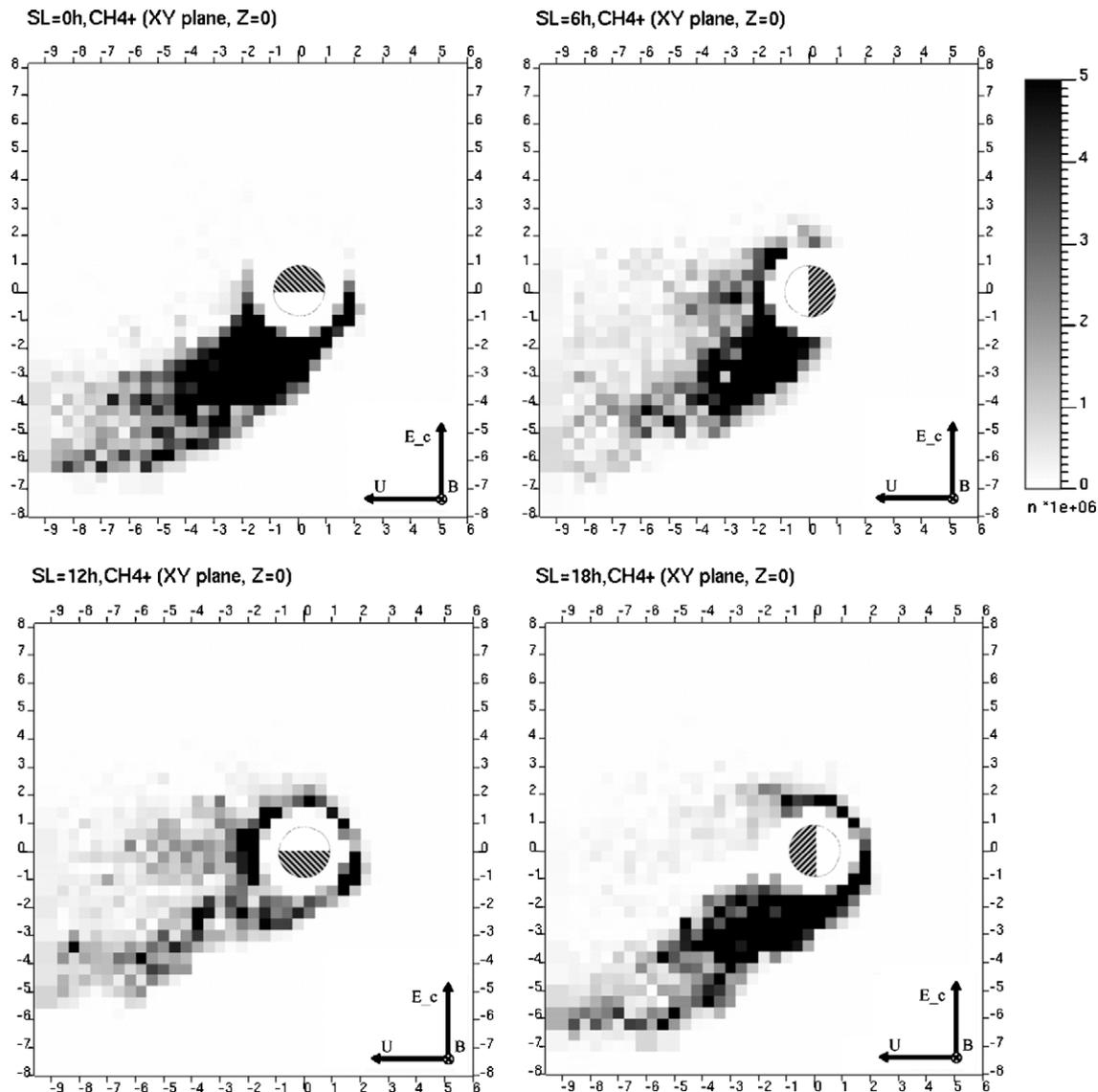Fig. 1. Number density of exospheric ions (CH_4^+) in four cases of different Saturn local time (SL). The scale on the axes is in R_T (= 2575 km), while the color bar is from 0 to 2×10^6 ions/m^3. The flow parameters are the same in all cases.
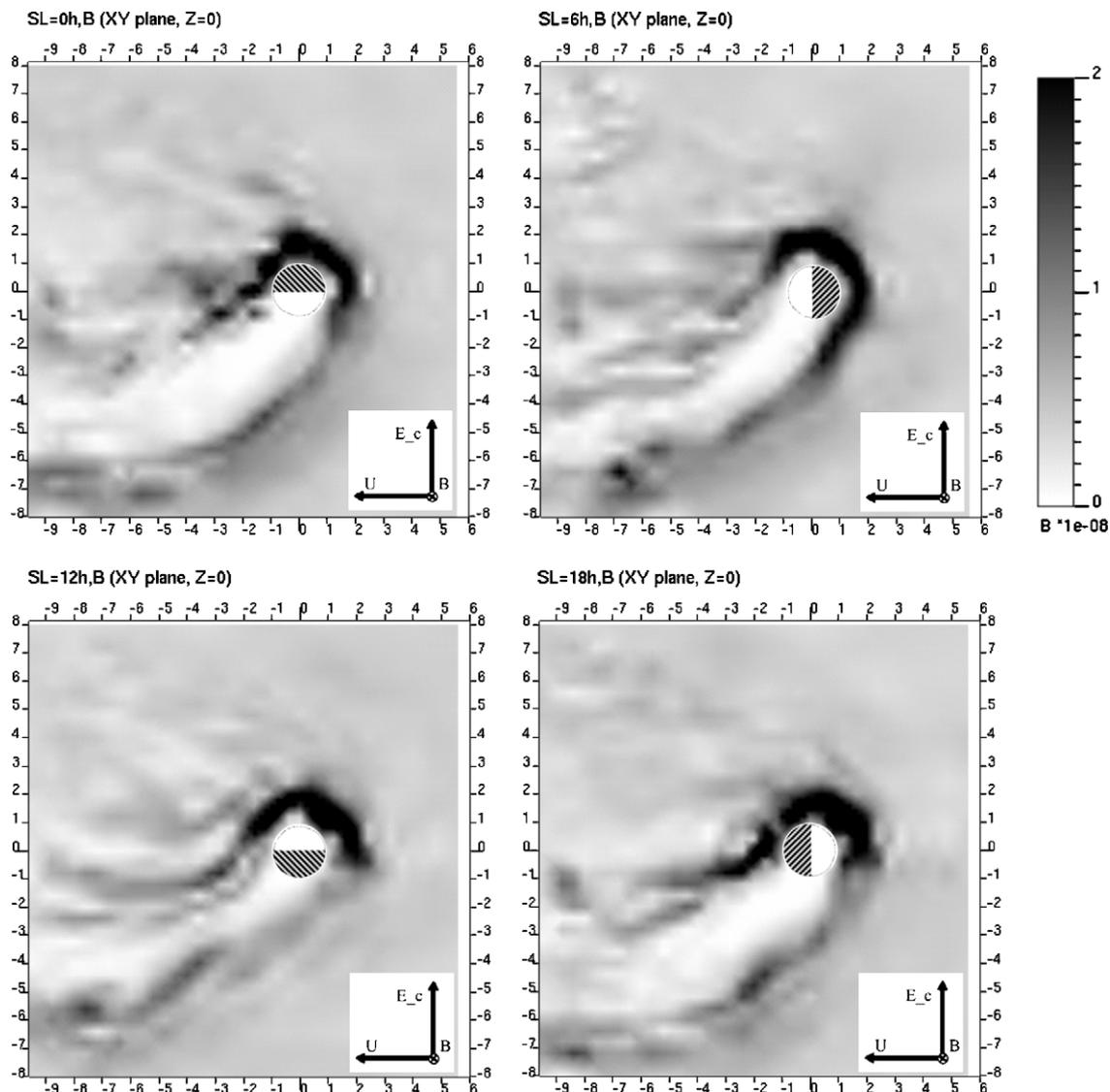
Fig. 2. Magnetic field around Titan in the orbital plane for four different Saturn local time. The values are smoothed with interpolation in all directions for clarity. The scale on the axes and the flow parameters are as in Fig. 1. The color bar goes from 0 to 20 nT.

cases are labeled according to the Saturn local time (SL) of the corresponding orbital position. The direction of the EUV shadow is shown with the shaded area on Titan and the views are limited to only the closest area around Titan as the number density quickly decreases with distance from Titan. In all panels vectors are shown for the flow direction (to the left), the magnetic field and the induced electric field E_C (in anti-Saturn direction). The case with no EUV shadow is not presented in the plots because that case does not correspond to a physical situation. Fig. 3 gives as an example a view of the general North–South symmetry in the ion density as well as in the total magnetic field for the SL = 12 case.

As seen in Fig. 1, the high density ionotail forms an angle of up to 45° towards Saturn from the flow direction. This tiltedness can be expected as the induced electric field accelerates emitted ions from Titan in the anti-Saturn direction, and the flow itself turns towards Saturn to con-

serve the momentum in the direction perpendicular to the undisturbed flow. This means that the wake is then turned towards Saturn, as was already seen in our preliminary study (Kallio et al., 2004).

The ion density in the tail is the highest in the SL = 0 case when the EUV is on the Saturn side of Titan. A large part of the CH_4^+ ions are formed on the Saturn side and consequently are not picked up by the flow, and a strong and much turned wake region is formed. On the other hand, the case SL = 12 has the least turning in the wake as the EUV source causes ionization on the anti-Saturn side, where the induced electric field quickly accelerates emitted ions more in that direction. This means that the deacceleration on the Saturn side is greatly reduced, and the tail is pressed more aligned with the flow. The general features of the other two cases are also reasonable; in the SL = 18 case the EUV comes from the direction of the flow and a lot of the ionized methane is picked up by the inci-
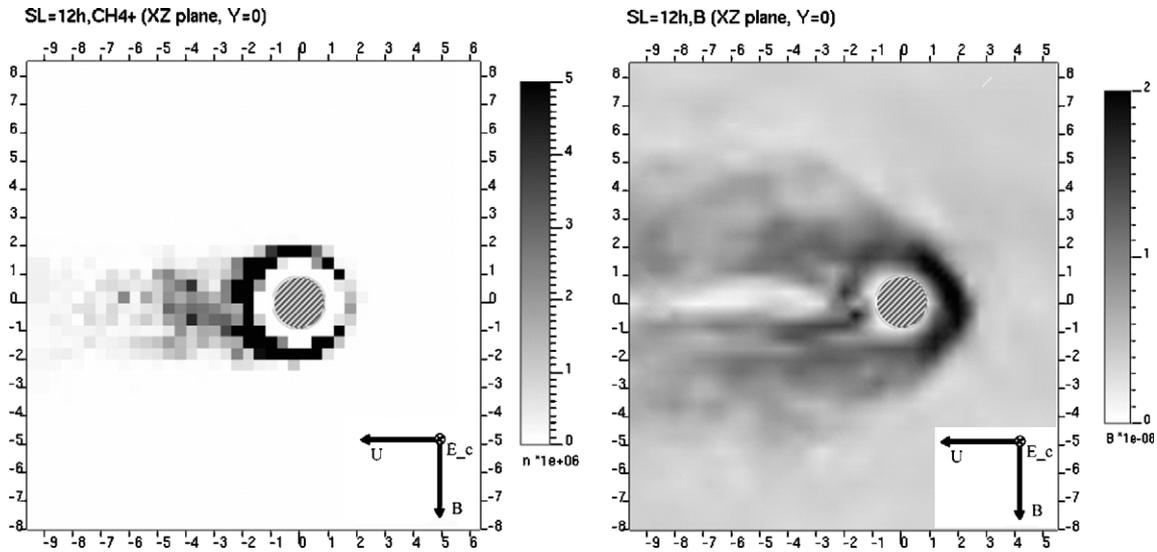
Fig. 3. Number density of ionospheric ions and the magnetic field around Titan in the plane parallel to the ideal corotational flow (in $-X$ direction) and the magnetic field ($-Z$) for the SL = 12 h case. Shadow would be in the direction of the viewer. Color bars and units of axes are as in Figs. 1 and 2.

dent flow and pushed around the obstacle of the conducting ionosphere together with the deflected magnetic field. Here the ion density remains much higher on the ramside so that also the magnetic barrier stays the furthest. In the SL = 6 case, the ionization takes place mainly in Titan's wake and the ionotail becomes the widest of all the cases, as a large portion of the ions is not directly influenced by the corotational flow. Here the magnetic barrier does not extend beyond Titan itself on the anti-Saturn side, whereas in the other cases the barrier is evident up to 4 Titan radii in the wake direction. The barrier is strong, however, on the Saturn side of Titan.

Naturally the N_2^+ ions are behaving much the same way as the methane ions; the only essential differences are the initial velocities and positions and the larger gyroradii. The patterns of the ion density of the N_2^+ species followed very closely those presented in Fig. 1 for CH_4^+. This comes about through the dominance of the photo-ionization; the ionospheric ion density is not enough to provide good shielding against the flow in areas where the photo-ionization does not take place.

The magnetic field plots in Fig. 2 show that the areas of weak magnetic field in the tail co-align with the ion density maxima. This anti-correlation comes about as the diamagnetic effect reduces the magnetic field greatly in the areas of high ion density. As the induced electric field is small where the magnetic field is weak, the ions experience no driving force to move them in these areas. The magnetic field maximum is close to the stagnation point of the corotational flow (seen from the flow lines – not presented) that is more on the anti-Saturn side than directly against the flow in all four cases. The magnetotail is clearly detectable up to $10 R_T$; the width follows the width of the high-density ion tail. An interesting feature, that is clearer in the SL = 0 and SL = 6 cases, is the intensified magnetic pile-up against the much-turned wake on the Saturn side. This pile-up forms due to the high ion density in the wake.

In Table 1 we present the net outflow of exospheric and ionospheric ion sources in the simulated cases. We also give the values for the case without the EUV shadow, that gives a kind of an upper value for the electron impact ionization in a case where the EUV shadow is on the wake side (i.e.,

Table 1
Net ion flow from Titan and impacting corotational flow to Titan

Saturn local time	CH_4^+ (exosphere)	N_2^+ (ionosphere)	Corotational flow
0	293 g/s (1.10)[a]	231 g/s (0.497)	21.2 g/s (0.133)
6	306 g/s (1.15)	235 g/s (0.506)	22.9 g/s (0.144)
12	294 g/s (1.11)	200 g/s (0.431)	21.3 g/s (0.133)
18	298 g/s (1.12)	183 g/s (0.393)	18.8 g/s (0.118)
No shadow[b]	464 g/s (1.75)	218 g/s (0.469)	17.0 g/s (0.107)

Values given both in units of g/s and 10^{25} ions/s. The number of ions created at the exospheric and ionospheric source were 2.0×10^{25} and 1.6×10^{25} ions/s or 532 and 744 g/s, respectively. A number, that the corotational flow impacts on Titan could be compared with, is the undisturbed flow through the obstacle cross cut $q = nU\pi R_0^2 = 1.97 \times 10^{24}$ ions/s ($R_0 = 4175$ km). This value equals the mass flux of 31.4 g/s. However, if the high thermal motion in the corotational plasma is taken into account, the flux through the obstacle boundary is significantly larger.
[a] Parenthesis the results are in units of 10^{25} ions/s.
[b] Shadowless case the emission of CH_4^+ is 814 g/s (3.06×10^{25} ions/s).

SL = 6, Keller and Cravens, 1994a). In that orbital position the electron impact ionization is expected to be the highest on the wake side as energetic electrons are led to the wake along the draped magnetic field lines. Included in Table 1 is also the flux of the corotational plasma impacting the absorbing obstacle boundary. However, there is not possible to say whether both hydrogen and nitrogen ions of the incident flow would behave the same way in impacting Titan's ionosphere or possibly much differently due to the factor of 14 difference in their gyroradii.

It seems remarkable that the net outflow of methane ions from Titan stays uniform with the different geometries. Even in the case with no shadow the fraction of escaping ions from the total number of methane ions emitted is the same 57%. A possible explanation for the uniformity of the photoion outflow might be that even though the area of photo-ionization changes, the fraction of ions with initial velocities pointing towards Titan stays the same. Thus, this fraction is very likely to change with the initial velocity distribution and the resolution near Titan. The gyroradius probably affects this only little with the small distance from the obstacle surface. The net emission of the ionospheric ions varies more even though a larger fraction of these ions are absorbed by the obstacle boundary. The SL = 0 and SL = 6 cases have higher outflow values than the rest. These are the cases where the tail is the strongest and the magnetically weak area the largest where the tail meets the obstacle boundary. This probably means that the ionospheric ions are able to escape from the tail side more easily as the gyroradius is large there. The net outflow is the least when SL = 18. Particular about this case is that the density of the methane ions is high almost all around the obstacle boundary. How exactly this inhibits the escape of the ionospheric ions would require more knowledge on the trajectories of individual particles. Same reason may explain why in the shadowless case the ionospheric emission is smaller than in those with strong tail structures (SL = 0 and 6) even though the iono- and magnetotails are significantly more extensive in this case (not shown).

The velocities of corotational ions form a wide spectrum around the bulk velocity due to the high temperature of the plasma. Thus, the deflection of the magnetic field around Titan's ionosphere only partly shields Titan from the corotational ions. SL = 18 is the case where the least amount of the ions of the incident flow are absorbed by the obstacle boundary. This is reasonable as in this case the magnetic barrier extends the furthest on the ramside effectively deflecting both the magnetic field and the corotating ions. The other three cases with shadow are very similar in this respect whereas in the shadowless case the shielding is naturally more effective when more ions are emitted around Titan.

4. Discussion

In the previous section we have presented results for the subsonic plasma interaction around Titan for four equatorial directions of the EUV source. Subsonic hybrid studies on Titan's interaction have been long due, but even at present day only few results exist. The importance of the hybrid simulations is in their capability to accurately model the drifts caused by the gyromotion of the ions which are ignored by MHD models. Thus our global hybrid simulation study with a subsonic corotational flow provides new insights to Titan's plasma interaction. Previous studies (Cravens et al., 1998; Kabin et al., 1999; Brecht et al., 2000; Kopp and Ip, 2001) have shown some of the features found also in this paper. These include the strong ionotail and the deflection of the corotational flow. However, the characteristics of the tiltedness of the tail structures toward Saturn are unprecedented results.

A preliminary comparison with the Voyager 1 data shows that the ion emission rates are at a correct level. The magnetic field profile for the Voyager 1 trajectory in the SL = 12 case was strikingly similar to the Voyager 1 measurement (SL was 13.5 h), including the short pass through the southern lobe and the peak of northward magnetic field (cf. Ness et al., 1982). However, the magnetic field in the SL = 18 case did not compare well with the Voyager 1 measurements, as the tail was much more shifted in the direction of Saturn.

This study of Titan's plasma environment is limited above the altitude of 1600 km from Titan's surface by the obstacle boundary employed by the simulation model. This seems like a good limit for a hybrid simulation that has no ion collision terms, since the exobase has been assumed to be somewhere around 1500–1600 km in altitude and above that the gases and plasma would be practically collisionless. What we have not considered is the temperature differences around the exosphere that in turn effect e.g. the altitude of the exobase. There are also recent results that imply that ion-neutral collisions may play a role higher up in the exosphere than previously thought (see Michell et al., 2005). These collisions could dampen the ion drifts and consequently the tilt of the tail might be less than in the model presented here.

Our model simulates the plasma environment of Titan in a simplified way. Results for all cases were very much symmetric in the North-South direction largely because there was nothing in the simulation to cause asymmetries in this direction. For example, the EUV source was in the plane of the orbit. Some way to implement the electron impact ionization in the model would be desirable, although it might to be secondary when compared with the photo-ionization. The assumption on the uniformity of the properties of the Kronian magnetosphere is clearly ideal (Wolf and Neubauer, 1982; Schardt et al., 1988; Hansen et al., 2000). Fortunately the characteristics of the magnetosphere are being revealed by the results from the Cassini spacecraft during its mission main phase in Saturn's system. We have already made preliminary runs with a two-species incoming plasma since including that important characteristic of the interaction is an obvious next step. Titan's exobase was represented by an absorbing and fully conducting sphere where the

emission of N_2^+ ions took place. Here the conductivity has become a concern, since there are expectations for the corotational magnetic field to be able to penetrate deep into the atmosphere, even below the surface of Titan (personal communication with Fritz Neubauer about recent MHD-modelling of Titan by his group). Also in our studies the ion emission at Titan seems not able to block the corotational magnetic field from reaching at least atmospheric altitudes in all cases. Introducing some resistivity in our obstacle could thus be important for the future versions of the simulation model. In this study it was also found that the edges of the ionotail can become narrow with high ion density drop. Therefore the electron pressure term we have so far ignored can have a measurable effect.

5. Summary

Using a hybrid code we have simulated the effects that the orbital position of Titan has on Titan's interaction with the corotational flow. We have assumed uniform magnetospheric properties throughout Titan's orbit and have found that orbital position has important effects on the tail structure. There are, however, several main features in the interaction that remain the same between the four cases studied: first, the tail always turns towards Saturn and magnetic wake co-aligns with the high-density ionotail. Second, the maximum of the magnetic field is close to the exobase boundary on the anti-Saturn side of Titan. The differences are found in the tilt angle and the ion density distribution of the tail, especially the amount of ions in the tail area varies in large degree. The net emissions from the exospheric and ionospheric sources vary only in a limited way. The fraction of the corotational ions reaching Titan's exopause was reduced when the ram direction and the Sun were on the same side (SL = 18), otherwise this corotational impact rate did not vary.

References

Amsif, A., Dandouras, D., Roelof, E.C. Modeling the production and the imaging of energetic neutral atoms from Titan's exosphere. J. Geophys. Res. 102 (A10), 169–181, 1997.

Blanc, M., Bolton, S., Bradley, J., et al. Magnetospheric and plasma science with Cassini-Huygens, in: Russell, C.T. (Ed.), The Cassini-Huygens Mission – Overview, Objectives and Huygens Instrumentarium. Kluwer Academic Publishers, Dordrecht, 2002 (also in Space Science Reviews, 104, 2002.).

Brecht, S.H., Luhmann, J.G., Larson, D.J. Simulation of the Saturnian magnetospheric interaction with Titan. J. Geophys. Res. 105, 13119–13130, 2000.

Coustenis, A., Salama, A., Schulz, B., Ott, S., Lellouch, E., Encrenaz, T.h., Gautier, D., Feuchtgruber, H. Titan's atmosphere from ISO mid-infrared spectroscopy. Icarus 161 (2), 383–403, 2003.

Cravens, T.E., Lindgren, C.J., Ledvina, S.A. A two-dimensional multifluid MHD model of Titan's plasma environment. Planet. Space Sci. 46, 1193–1205, 1998.

Hansen, K.C., Gombosi, T.I., DeZeeuw, D.L., et al. A3D global MHD simulation of Saturn's magnetosphere. Adv. Space Res. 26, 1681–1690, 2000.

Hartle, R.E., Sittler Jr., E.C., Ogilvie, K.W., et al. Titan's ion exosphere observed from Voyager 1. J. Geophys. Res. 87, 1383–1394, 1982.

Huebner, W.F., Keady, J.J., Lyon, S.P. Solar photo rates for planetary atmospheres and atmospheric pollutants. Astrophys. Space Sci. 195, 1–294, 1992.

Kabin, K., Gombosi, T.I., DeZeeuw, D.L., et al. Interaction of the Saturnian magnetosphere with Titan: results of a three dimensional MHD simulation. J. Geophys. Res. 104, 2451–2458, 1999.

Kabin, K., Israelevich, P.L., Ershkovich, A.I., et al. Titan's magnetic wake: atmospheric or magnetospheric interaction. J. Geophys. Res. 105, 10761–10770, 2000.

Kallio, E., Janhunen, P. Atmospheric effects of proton precipitation in the Martian atmosphere and its connection to the Mars-solar wind interaction. J. Geophys. Res. 106 (A4), 5617–5634, 2001.

Kallio, E., Janhunen, P. Ion escape from Mars in a quasineutral hybrid model. J. Geophys. Res. 107(A3), 2002, doi:10.1029/2001JA000090.

Kallio, E., Sillanpää, I., Janhunen, P. Titan in subsonic and supersonic flow. Geophys. Res. Lett. 31, L15703, 2004, doi:10.1029/2004GL020344.

Keller, C.N., Cravens, T.E., Gan, L. A model of the ionosphere of Titan. J. Geophys. Res. 97, 12117–12135, 1992.

Keller, C.N., Cravens, T.E. One-dimensional multispecies hydrodynamic models of the wakeside ionosphere of Titan. J. Geophys. Res. 99 (A4), 6527–6536, 1994a.

Keller, C.N., Cravens, T.E., Gan, L. One-dimensional multispecies magnetohydrodynamic models of the ramside ionosphere of Titan. J. Geophys. Res. 99, 6527–6536, 1994b.

Kopp, A., Ip, W.-H. Asymmetric mass loading effect at Titan's ionosphere. J. Geophys. Res. 106, 8323–8332, 2001.

Ledvina, S.A., Luhmann, J.G., Cravens, T.E. Ambient ion distributions in Saturn's magnetosphere near Titan during a non-Voyager type interaction. Adv. Space Res. 33, 221–226, 2004.

Lellouch, E., Coustenis, A., Sebag, B., Cuby, J-G., Lpez-Valverde, M., Schmitt, B., Fouchet, T., Crovisier, J. Titan's 5 μm window: observations with the Very Large Telescope. Icarus 162 (1), 125–142, 2003.

Michell, D.G., Brand, P.C., Roelof, E.C., Dandouras, J., Krimigis, S.M., Mauk, B.H. Energetic neutral atom emissions from Titan interaction with Saturn's Magnetosphere. Science 308, 989–992, doi:10.1126/science.1109805, 2005.

Nagy, A.F., Liu, Y., Hansen, K.C., et al. The interaction between the magnetosphere of Saturn and Titan's ionosphere. J. Geophys. Res. 106, 6151–6160, 2001.

Ness, N.F., Acuna, M.H., Behannon, K.W. The induced magnetosphere of Titan. J. Geophys. Res. 87, 1369–1381, 1982.

Neubauer, F.M., Gurnett, D., Scudder, J.D., et al. Titan's magnetospheric interaction, in: Gehrels, T., Matthews, M.S. (Eds.), Saturn. The University of Arizona Press, Tucson, Arizona, 1988.

Roe, H.G., de Pater, I., McKay, C.P. Seasonal variation of Titan's stratospheric ethylene (C2H4) observed. Icarus 169 (2), 440–461, 2004.

Schardt, A.W., Behannon, K.W., Lepping, R.P., et al. The outer magnetosphere, in: Gehrels, T., Matthews, M.S. (Eds.), Saturn. University of Arizona Press, pp. 416–459, 1988.

Wolf, D.A., Neubauer, F.M. Titan's highly variable plasma environment. J. Geophys. Res. 87, 881–885, 1982.